applied sciences

MDPI

Article

A New Approach for Predicting the Rheological Properties of Oil-Based Drilling Fluids under High Temperature and High Pressure Based on a Parameter-Free Method

Yuguang Ye [1,*], Honghai Fan [1] and Yuhan Liu [2]

[1] School of Petroleum Engineering, China University of Petroleum, Beijing 102249, China
[2] CNPC Engineering Technology Research and Development Company Limited, Beijing 100007, China
* Correspondence: 2018312011@student.cup.edu.cn

Abstract: Under different temperatures and pressures, the physical parameters of drilling fluid will change, resulting in inaccurate drilling hydraulic calculations. Aiming to address the problem of the traditional rheological prediction method needing to first determine the rheological model, this paper proposed a method for first predicting the readings of the rheometer and then determining the rheological model. The model established in this paper adopted a parameter-free method, which expands the application range of the model. Rheology experiments were carried out on the three types of oil-based drilling fluids collected at the well site. The model in this paper was verified based on the experimental data. The results showed that, compared with the traditional drilling fluid rheological prediction method, the model established in this paper had a better prediction effect, with an average error of 4.85%, and the average error reduction ranges from 3.8% to 8.3%. The model established in this paper is able to provide theoretical support for accurate hydraulic calculation.

Keywords: HTHP; oil-based drilling fluid; rheology; parameter-free method; managed pressure drilling

Citation: Ye, Y.; Fan, H.; Liu, Y. A New Approach for Predicting the Rheological Properties of Oil-Based Drilling Fluids under High Temperature and High Pressure Based on a Parameter-Free Method. *Appl. Sci.* **2023**, *13*, 8592. https://doi.org/10.3390/app13158592

Academic Editors: José M. Franco, Jean-Michel Guenet, Qingbang Meng, Yingrui Bai, Bin Liang and Xiaocong Lyu

Received: 27 April 2023
Revised: 15 July 2023
Accepted: 24 July 2023
Published: 26 July 2023

1. Introduction

With the development of technology, deep and ultra-deep layers have gradually become one of the important directions of current exploration and development. With developments in drilling, the temperature and pressure in the formation are becoming higher and higher, and the rheology of the drilling fluid changes with the temperature and pressure. The rheology of the drilling fluid measured only by the surface conditions cannot accurately represent the true situation of the drilling fluid rheology in the wellbore, which seriously affects the calculation accuracy of drilling hydraulics. Therefore, it is necessary to study the rheological changes in the drilling fluid under high-temperature and high-pressure conditions [1,2].

The study of the rheological properties of drilling fluids at high temperature and high pressure in order to accurately calculate the hydraulic parameters of drilling fluid began in the 1950s, but it was mainly concentrated on the Bingham model and the power law model, and there was no systematic calculation method of rheological parameters at high temperature and high pressure. In 1958, Srini Vasan and Gatlin used a Fann V-G viscometer to analyze the rheology of clay-based drilling fluids at different temperatures and constructed a simple prediction model of the plastic viscosity of drilling fluid [3]. In 1967, Annis conducted an experimental study on the rheology of water-based drilling fluids at high temperature and high pressure using Fann's high-temperature and high-pressure viscometer and presented a qualitative analysis of the yield value and viscosity change in drilling fluid at high temperature and high pressure [4]. In 1975, McMordie et al. conducted relevant research on the rheology of oil-based drilling fluids at high temperature and high pressure based on the power law model. In the analysis process, the logarithm of both sides of the power law model was converted into a linear model. At the same time, it was assumed that the temperature and pressure only affected the consistency coefficient of the drilling fluids and the liquidity index had no effect. From this, a simple prediction model of the consistency coefficient was obtained [5]. In 1985, Polite used the Bingham model to carry out an experimental analysis of the rheological properties of reverse-emulsified oil-based drilling fluids under high temperature and pressure and presented a prediction model of the Bingham yield value and plastic viscosity [6]. Since then, many researchers have carried out corresponding research and analysis on the high-temperature and high-pressure rheology of drilling fluid, but most of these studies are based on the Bingham and power-law rheological models recommended by the American Petroleum Institute (API), and the corresponding rheological parameter regression models are obtained through rheological experiment regression. In 1989, Yan Jienian carried out an experimental analysis on the high-temperature and high-pressure rheology of mineral-oil-based drilling fluids with different densities and conventional water-in-oil emulsion drilling fluids, mainly analyzing the changes in the plastic viscosity, apparent viscosity, and yield value of drilling fluids with under different temperatures and pressures [7]. In 1990, Yan Jienian presented a prediction model for the apparent viscosity of water-in-oil emulsion drilling fluids [8]. In 2009, Zhao Shengying and others improved the model and further proposed a comprehensive mathematical model for predicting plastic viscosity, yield value, and apparent viscosity [9]. In the same year, Zhao Huaizhen and others carried out an experimental study on the ultra-high-temperature and high-pressure rheology of high-temperature water-based drilling fluids and presented a mathematical model for predicting the apparent viscosity of the drilling fluids [10]. In 2010, Wang Fuhua studied the apparent viscosity and plastic viscosity of water-based drilling fluids and established a model for the variation of apparent viscosity with temperature and pressure [11]. In 2017, Gokdemir conducted research on water-based drilling fluids using a high-pressure, high-temperature (HPHT) Anton Paar MCR-302 compact rheometer, analyzing the effects of pressure on yield stress, apparent viscosity, and the flow behavior index [12]. In 2018, FAKOYA established a model for the apparent viscosity change of oil-based mud based on its characteristics [13]. In 2018, Anawa compared the error of different drilling fluid rheological models in predicting the rheological properties of bentonite drilling fluid [14]. In 2021, Cesar Vivas conducted a study on the thermal stability of drilling fluids under high temperature and pressure [15]. In 2021, Agwu systematically reviewed recent research on the prediction of the high-temperature and high-pressure rheological properties of drilling fluids [16]. In 2021, Okorie conducted research on the rheological properties of high-temperature and high-pressure drilling fluids, summarizing the laboratory, field, and model studies used in the research process [17]. In 2023, Alade studied the effect of high temperature and pressure on the rheological properties of drilling fluids using CFD methods [18].

To sum up, the rheological analysis of drilling fluid at high temperature and high pressure is mostly based on Bingham and power law models, and the rheological parameter prediction models given by experiments are mostly empirical formulas. The method first assumes the rheological model and then introduces the variable temperature T and pressure P to modify and calculate the rheological parameters at high temperature and high pressure. These models are based on the empirical formula of high-temperature and high-pressure rheological parameters and temperature and pressure (or temperature and pressure changes); that is, the empirical formula is fitted with experimental data to predict the specific rheological parameters (such as plastic viscosity, apparent viscosity, etc.) of drilling fluid at different temperatures and pressures.

This method has the following shortcomings: due to the possibility of changes in the most suitable rheological model of drilling fluid at different temperatures and pressures, determining the rheological model before prediction may cause significant errors.

In view of this problem, this paper predicts the readings of the six-speed viscometer of the high-temperature and high-pressure oil-based drilling fluid and then determines the rheological model and parameters of the temperature based on the predicted readings of the viscometer, which improves the prediction accuracy of the rheology of the high-temperature and high-pressure oil-based drilling fluid and provides the basis and help for the subsequent hydraulic calculation.

2. Rheology Experiment on Oil-Based Mud

2.1. Experimental Equipment

Due to the different formulations of different drilling fluids, the rheological changes in drilling fluids under high temperature and high pressure are also different. Therefore, it is difficult to predict the rheological properties of drilling fluids under high temperature and high pressure for all drilling fluids. It is necessary to carry out indoor experiments for different drilling fluids and then select an appropriate method for rheological prediction.

In the laboratory test, the readings of the six-speed viscometer of the drilling fluid were measured, and the corresponding rheological parameters were regressed according to the corresponding rheological model.

The Grace M8500 high-temperature and high-pressure rheometer was used in this experiment, and the basic parameters of the equipment are shown in Table 1.

Table 1. Equipment parameter.

Equipment Parameters	Parameter Range
Rotating speed	0–600 rpm
Temperature	Room temperature–600 °F
Pressure	atm–30,000 psi
Viscosity	0.5–5,000,000 cP

2.2. Experimental Design

In this paper, the oil-based mud used in the actual drilling of three wells was collected at the well site. The three types of oil-based mud experimental test samples are shown in Table 2.

Table 2. High-temperature and high-pressure rheological test samples.

Sampling Well	Mud Type	Mud Density	Mud Oil-Water Ratio
Well Hu 6	Diesel-based	1.97	85/15
Well Tianan 1	white oil base	2.26	89/11
Well Tianwan 1	white oil base	2.18	90/10

We measure the data of the viscometer at 3, 6, 100, 200, 300, and 600 speeds in the range of 60 °C to 160 °C and 0.1 MPa to 150 MPa.

2.3. Experimental Result

Experiments were carried out on the three samples. Based on the experimental plan, the results from the Tianan 1 well are shown in Figure 1.

Based on the experimental plan, the results from the Tianwan 1 well are shown in Figure 2.

The results from the Hu 6 well are shown in Figure 3.

It can be seen from the figure that as the temperature increases, the shear stress shows a downward trend. When the temperature is increased from 60 °C to 100 °C, the shear stress value decreases by 40–52% at a shear rate of 1021.92 s^{-1}. The higher the pressure, the greater the shear stress reduction. As the pressure increases, the shear stress gradually increases. When the pressure is low, the increase in shear stress is small.

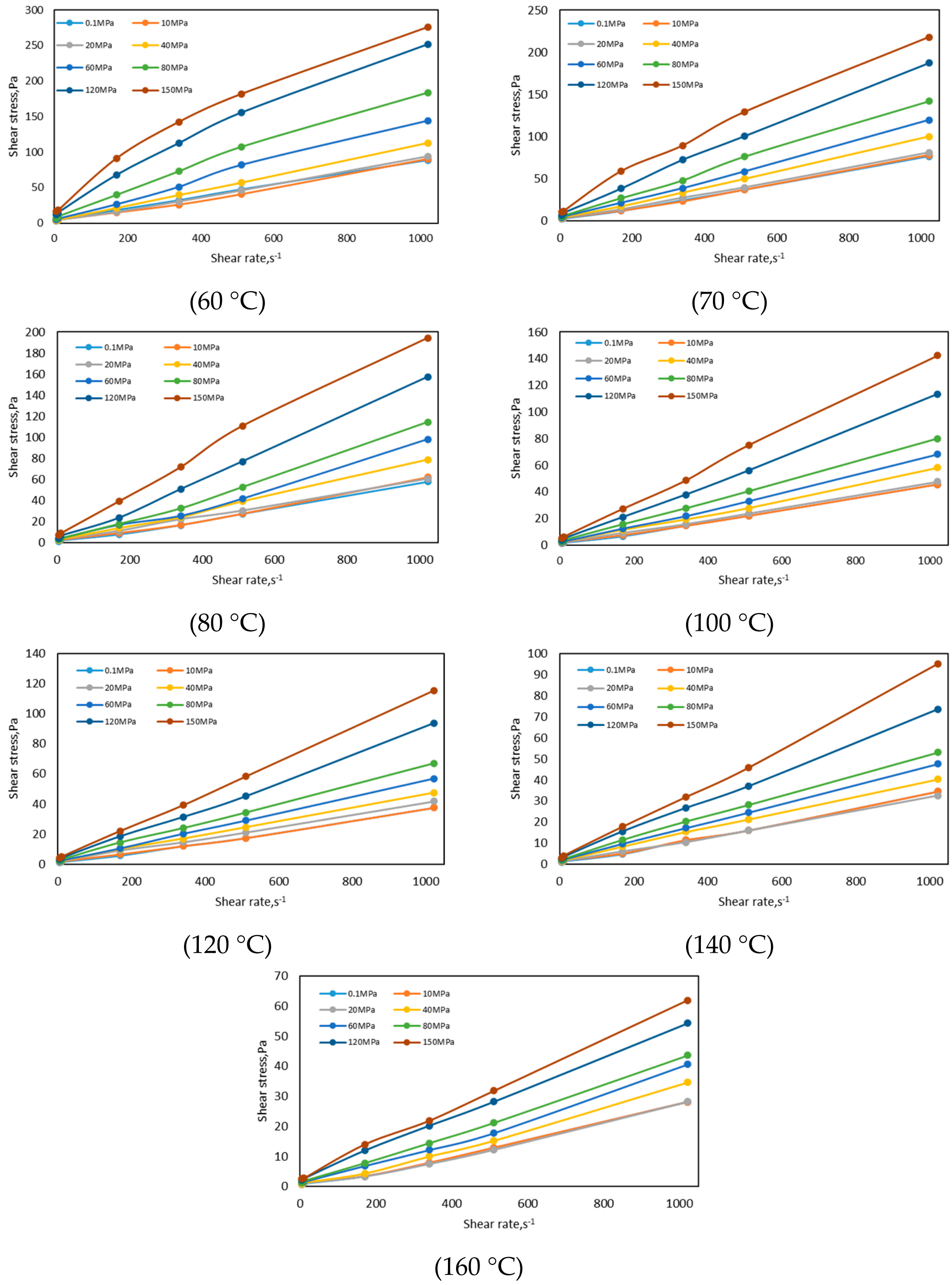

Figure 1. Variation in rheological curve with temperature in the Tianan 1 Well.

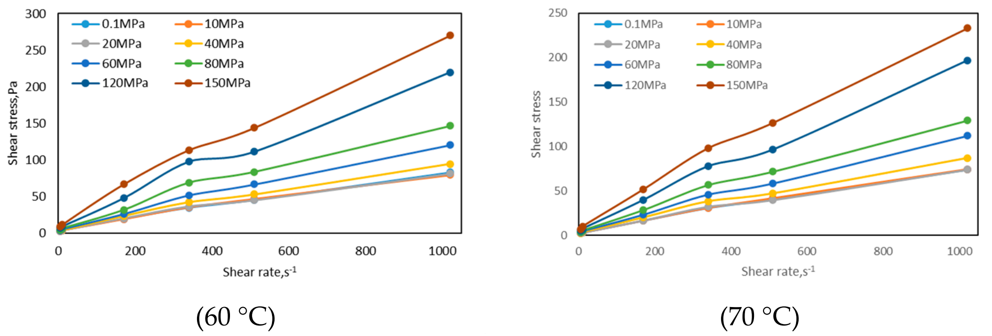

Figure 2. *Cont.*

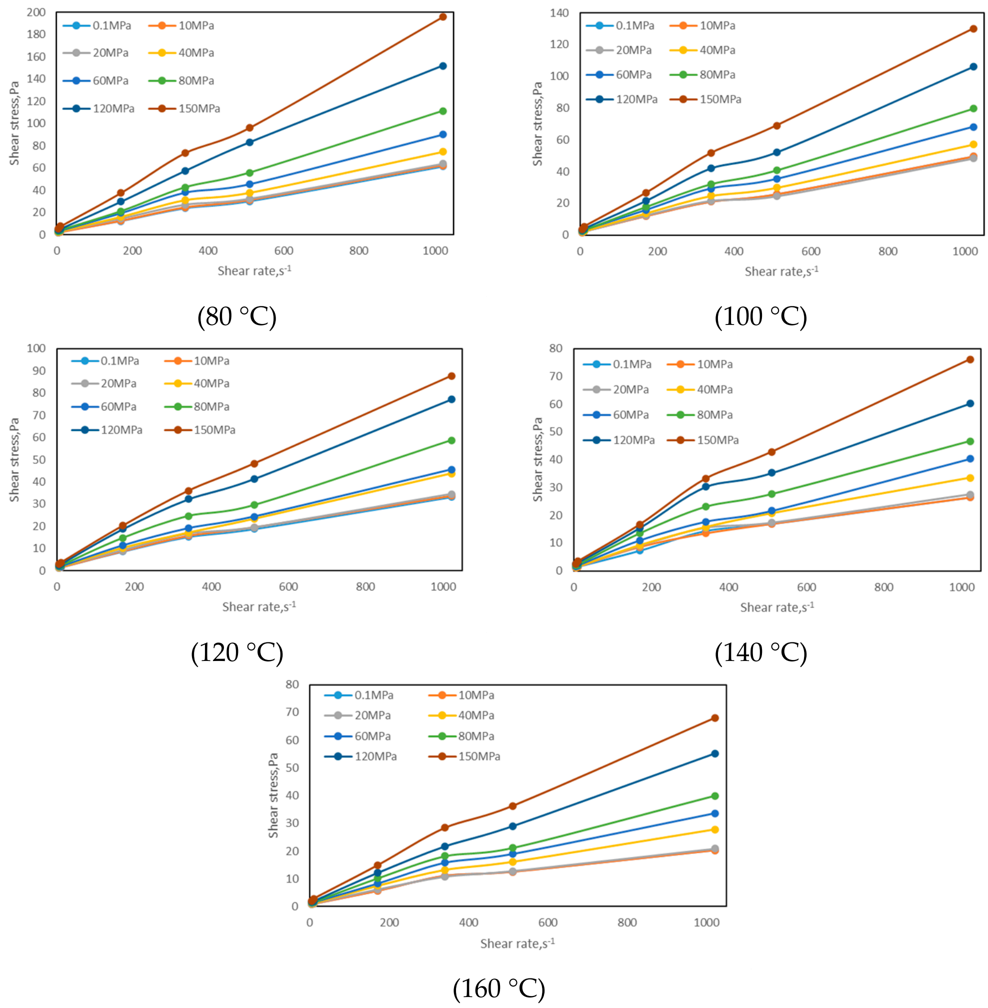

Figure 2. Variation in rheological curve with temperature in the Tianwan 1 Well.

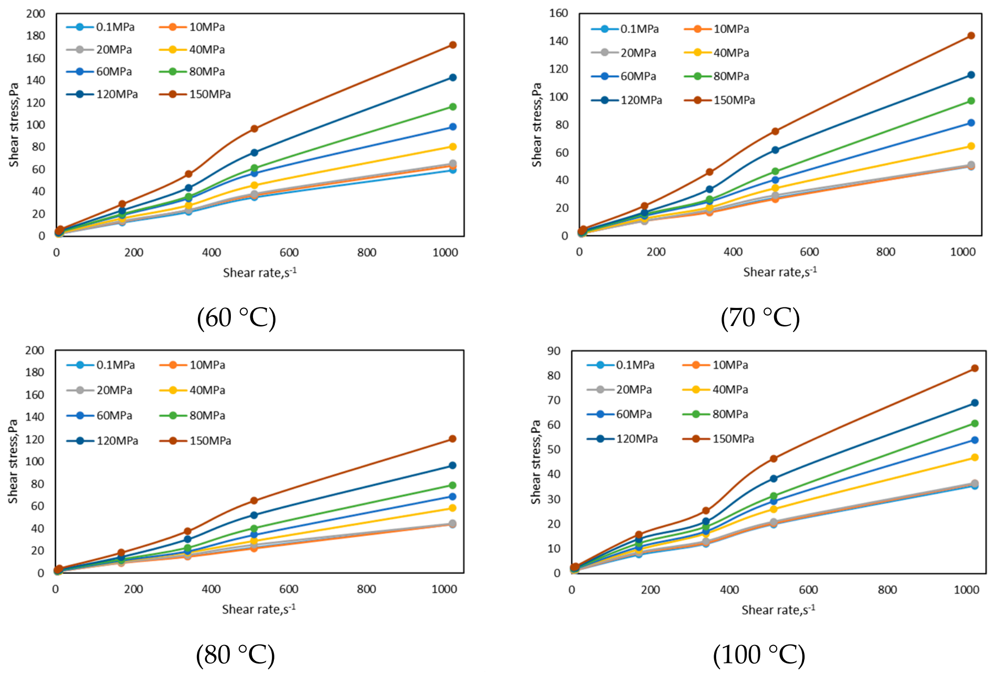

Figure 3. *Cont.*

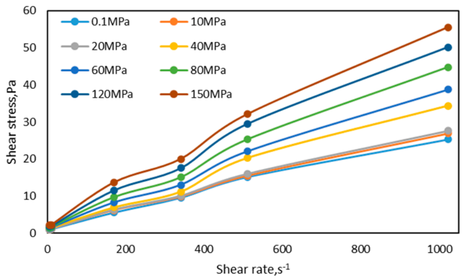

(120 °C)

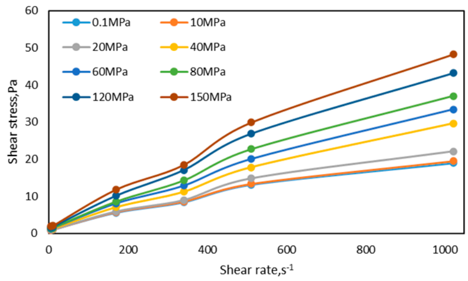

(140 °C)

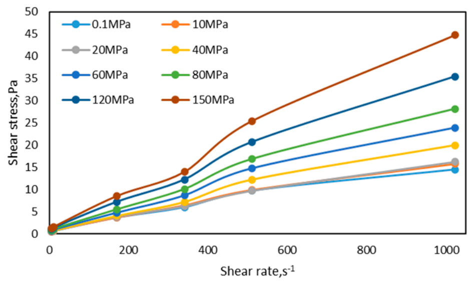

(160 °C)

Figure 3. Variation in rheological curve with temperature in the Hu 6 well.

3. Model Establishment

At present, the traditional method for predicting the rheological properties of drilling fluids under high temperature and high pressure first needs to determine the rheological model and then calculate the rheological parameters under the experimental conditions, and finally perform regression analysis on the rheological parameters to obtain the prediction of the rheological properties of drilling fluids under high temperature and high pressure. However, under different temperature and pressure conditions, the drilling fluid may conform to different rheological models, and inappropriate rheological models will increase the error of hydraulic calculation. Aiming to address this problem, this paper proposed a method to directly predict the results of rheological experiments.

3.1. Model Building

The rheological model is an important method for describing the rheology of drilling fluid. Rheological parameters in rheological model can be calculated based on readings from a six-speed rotational viscometer. Therefore, if the readings of the six-speed rotational viscometer of the drilling fluid under different temperature and pressure conditions can be obtained, then the rheological parameters under the corresponding conditions can be calculated to determine the rheological properties of the drilling fluid under different temperatures and pressures. It is impractical to experimentally obtain rheometer readings at all temperatures and pressures. Therefore, this paper establishes a predictive viscometer reading model to obtain rheometer readings at any specified temperature. After determining the shear stress values at a set of six rotational speeds, the rheological parameters of different rheological models can be determined via regression. The conversion relationship between the rotational speed and the reading of a six-speed viscometer in terms of shear rate and shear stress is as follows:

$$\tau = 0.511\theta \tag{1}$$

$$\gamma = 1.7032\text{N} \tag{2}$$

where τ is the shear stress (Pa), γ is the shear rate (1/s), θ is the reading of a six-speed viscometer (lb/100 ft2), and N is the rotational speed (1/min).

Therefore, a prediction of a six-speed viscometer reading is a prediction of shear stress at a given shear rate. After obtaining the predicted six-speed viscometer readings under a certain temperatures and pressures, the rheological model can be selected and the corresponding rheological parameters can be determined.

Since the variation in shear stress with temperature and pressure is different at different rotational speeds, corresponding prediction models need to be established.

The accuracy of nonlinear regression is greatly affected by the regression function. However, different drilling fluids may conform to different regression functions. This paper uses a parameter-free method for regression to expand the application range of the model. Parameter-free models do not make any special assumptions regarding the regression function, which makes them more flexible in terms of reducing bias.

Weighted linear regression, which introduces a weight function into the traditional linear regression model, was adopted in this paper. The mathematical expression for weighted linear regression is as follows:

$$\mathrm{y} = \varphi \cdot \mathrm{x} \tag{3}$$

The coefficient matrix φ of the prediction point can be calculated via the following formula:

$$\varphi = \left(\mathrm{X}^{\mathrm{T}}\mathrm{W}\mathrm{X}\right)^{-1}\mathrm{X}^{\mathrm{T}}\mathrm{W}\mathrm{Y} \tag{4}$$

where Y is the measured data and W is the weight coefficient; the weight function in this article uses a Gaussian kernel function. The Gaussian kernel function is a matrix with non-zero diagonal data only, and the expression of the Gaussian kernel function is as follows:

$$w_{i,i} = e^{\left(-\frac{||x-x_i||}{2\sigma}\right)} \tag{5}$$

where σ is the weight ratio, x is the temperature and pressure of the prediction point, and x_i is the temperature and pressure of the actual data point.

After inputting the temperature and pressure conditions that need to be predicted, the corresponding weight coefficient and coefficient matrix can be calculated to obtain the prediction readings under this condition.

After obtaining the readings of the six-speed viscometer under the predicted temperature and pressure conditions, the rheological model of the drilling fluid can be determined through the traditional rheological model optimization method and the corresponding rheological parameters can be calculated.

For the problem studied in this article, the independent variables are the temperature and pressure values of the predicted point. The dependent variable is the shear stress value at the corresponding shear rate at the predicted point. In this article, there are 56 sets of experiments with the same shear rate, among which 14 sets of data with a pressure of 40 MPa and a temperature of 70 °C were selected as test data. Due to the presence of constant terms, the dimensions of each matrix are shown in Table 3.

Table 3. Matrix meaning and matrix dimensions.

Matrix	Matrix Meaning	Dimensions
x	independent variable	(3, 1)
φ	coefficient matrix	(3, 1)
y	dependent variable	(1, 1)
X	experimental condition	(42, 3)
W	weight coefficient	(42, 42)
Y	experimental measurement results	(42, 1)

3.2. Examples of Shear Stress Prediction

Changes in the value of independent variables can also cause changes in the weight matrix and coefficient matrix. Therefore, the model established in this article does not have a determined weight coefficient and a coefficient matrix. The matrix results of listing 14 test sets contain a huge amount of data, with the weight matrix of only 14 groups having a data volume of 3528. Therefore, this article takes the drilling fluid of the Tianan 1 well as an example under the conditions of 40 MPa, 70 °C, and a rotational speed of 600 rpm, and provides all matrix results.

As shown in Table 4, the prediction condition is 40 MPa, 70 °C, a constant item 1 is added to the independent variable matrix, and the measured result of the dependent variable is 100.064.

Table 4. Value of independent variables and experimental measurement results.

	x		y_Measured
1	70	40	100.064

Based on Table A1 in Appendix A, the data of the experimental condition matrix X and the experimental result Y were extracted, and the values on the diagonal of the weight matrix were calculated based on the input data and X, Y. The results are shown in Table 5.

Table 5. Value of experimental condition matrix, experimental result matrix, and weight coefficient matrix.

	X		Y	$w_{i,i}$
1	60	0.1	173.61	3.17×10^{-8}
1	60	10	177.25	3.70×10^{-5}
1	60	20	183.72	6.08×10^{-3}
1	60	60	281.88	6.08×10^{-3}
1	60	80	359.02	2.93×10^{-8}
1	60	120	492.5	1.57×10^{-29}
1	60	150	540.16	8.61×10^{-55}
1	80	0.1	113.35	3.17×10^{-8}
1	80	10	121.63	3.70×10^{-5}
1	80	20	118.72	6.08×10^{-3}
1	80	60	192.16	6.08×10^{-3}
1	80	80	224.3	2.93×10^{-8}
1	80	120	308.11	1.57×10^{-29}
1	80	150	380.09	8.61×10^{-55}
1	100	0.1	89.15	9.05×10^{-12}
1	100	10	89.18	1.05×10^{-8}
1	100	20	93.03	1.73×10^{-6}
1	100	60	133.29	1.73×10^{-6}
1	100	80	156.49	8.34×10^{-12}
1	100	120	221.84	4.46×10^{-33}
1	100	150	278.37	2.45×10^{-58}
1	120	0.1	73.44	7.34×10^{-19}
1	120	10	73.54	8.56×10^{-16}
1	120	20	81.91	1.41×10^{-13}
1	120	60	111.29	1.41×10^{-13}
1	120	80	131.17	6.77×10^{-19}
1	120	120	183.46	3.62×10^{-40}
1	120	150	225.56	1.99×10^{-65}
1	140	0.1	67.7	1.70×10^{-29}
1	140	10	67.8	1.98×10^{-26}
1	140	20	63.86	3.26×10^{-24}
1	140	60	93.31	3.26×10^{-24}
1	140	80	103.74	1.57×10^{-29}
1	140	120	143.81	8.38×10^{-51}

Table 5. *Cont.*

	X		*Y*	$w_{i,i}$
1	140	150	186.21	4.60×10^{-76}
1	160	0.1	54.96	1.12×10^{-43}
1	160	10	55.06	1.31×10^{-40}
1	160	20	55.28	2.15×10^{-38}
1	160	60	79.58	2.15×10^{-38}
1	160	80	85.43	1.03×10^{-43}
1	160	120	106.37	5.52×10^{-65}
1	160	150	121.21	3.03×10^{-90}

The coefficient matrix φ calculated based on the experimental condition matrix X, experimental result matrix Y, and weight matrix W are shown in Table 6.

Table 6. Coefficient matrix and prediction results.

	φ		*y*
378.99	−3.863	2.140	99.228

The prediction result of the prediction method established in this article is 99.228, and the actual measurement result is 100.084, with a relative error of 0.85%.

Similarly, the shear stress values of other rotational speeds can be calculated using the above process.

3.3. Parameter Determination

When the value of σ is different, the image of the Gaussian kernel function is also different. Figure 4 shows the image of the Gaussian kernel function when the value of σ is different.

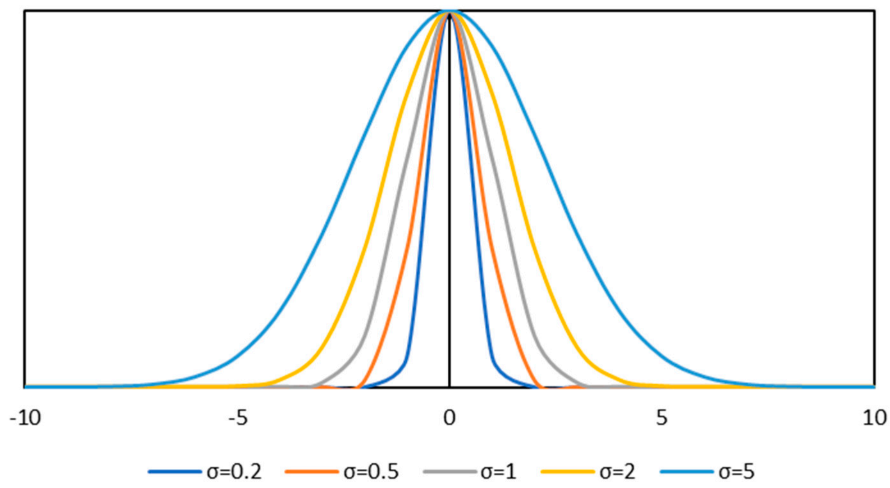

Figure 4. Gaussian kernel function image under different σ values.

It can be seen from the figure that the larger the value of σ, the wider the Gaussian kernel function. When the value of σ is larger, more data are used in the regression, and when σ is too large, the curve-fitting effect decreases. When the value of σ is small, the data used for the regression are closer to the prediction point, but a too-small σ value leads to the overfitting of the curve.

Therefore, by choosing an appropriate value for σ, the fitting effect of the weighted linear regression can be effectively improved.

If all regression data are directly used to verify the prediction results, the error of the model prediction is very low, and the impact of the model on non-measured values cannot be verified. Therefore, this paper extracted the data from 40 MPa of pressure and a temperature of 70 °C and did not participate in the regression of the model. We compared the advantages and disadvantages of each model through the performance of the model in two groups of non-training sets.

The average error of the model can be calculated using the following formula:

$$\text{Erro} = \frac{1}{n}\sum_{i=1}^{n}\frac{\left|y_i^* - y_i\right|}{y_i} \tag{6}$$

where y_i^* is the predicted value and y_i is the measured value.

Taking the rheological experimental data of the Tianan 1 well as an example, the appropriate sigma value can be selected through the method of minimum average error.

After obtaining experimental data, the average error of the prediction method was calculated for sigma values between 0.1 and 1, with an interval of 0.1. The relative error is shown in Figure 5.

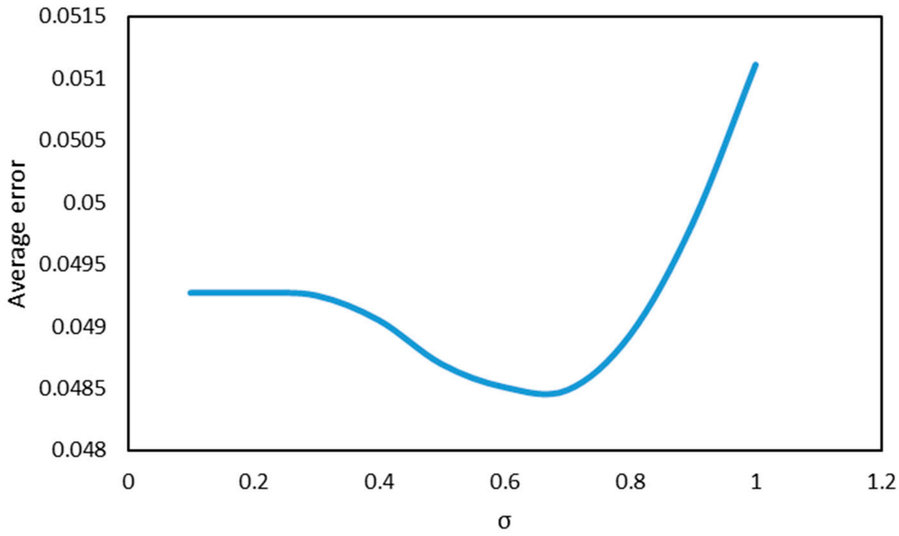

Figure 5. Comparison of average error under different σ values.

It can be seen from Figure 5 that the overall average error decreases first and then increases with the increase in the value of σ. This is because when the value of σ is too large, the fitting of the curve is not good enough. When the value of σ is too small, the curve is overfitted, and the prediction performance for non-datasets is reduced. When σ is 0.7, the overall error is the smallest, so 0.7 is the optimal value.

The relationship between the measured value and the predicted value of the model at each speed when the value of σ is 0.7 is shown in Figure 6.

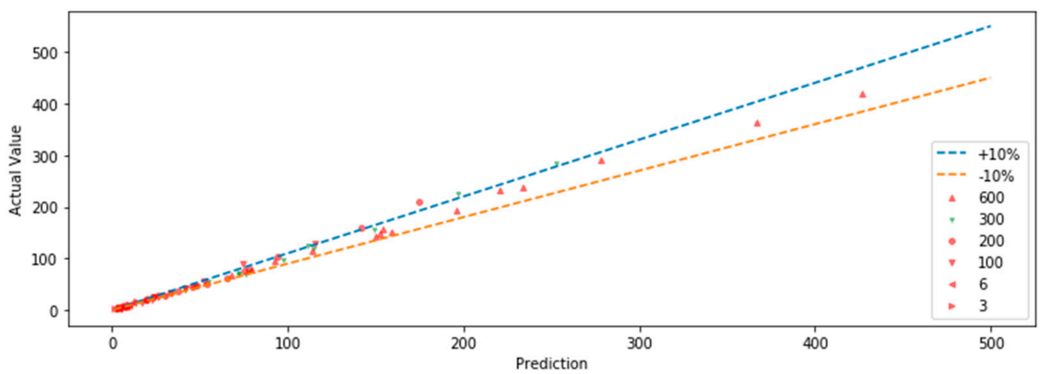

Figure 6. Comparison between predicted value and actual value (σ = 0.7).

It can be seen from the figure that the error between the predicted value and the true value of the readings for each rotating speed is predominantly within ±10%, and only the individual abnormal points with rotating speeds of 200 and 300 have large errors. The model established in this paper has a good prediction effect on the readings of the drilling fluid viscometer.

3.4. Rheological Prediction

The prediction method of shear stress at each speed is established above. Based on the prediction results, the rheological mode and rheological parameters at a specified temperature and pressure can be determined via regression. The prediction process of drilling fluid rheology is as follows:

(1) (Measure or collect the six-speed viscometer data of the drilling fluid that need to be predicted;
(2) Determine the temperature and pressure that need to be predicted;
(3) Calculate the weight matrix of 3 rpm, 6 rpm, 100 rpm, 200 rpm, 300 rpm, and 600 rpm under the specified temperature and pressure conditions based on Formula (5);
(4) Calculate coefficient matrices of 3 rpm, 6 rpm, 100 rpm, 200 rpm, 300 rpm, and 600 rpm under specified temperature and pressure conditions based on Formula (4);
(5) Calculate the readings of 3 rpm, 6 rpm, 100 rpm, 200 rpm, 300 rpm, and 600 rpm under the specified temperature and pressure conditions based on Formula (3);
(6) Based on Formulas (1) and (2), convert the rotational speed and reading into shear rate and shear stress;
(7) Based on the predicted results, the rheological parameters and corresponding errors of rheological models, such as the Bingham model, power law model, and H-B model, are calculated using the regression method;
(8) By comparing the errors, select the rheological model with the smallest error as the rheological model under the temperature and pressure.

3.5. Example of Rheological Prediction

Based on the experimental data results of the Tianan 1 well, after removing the 40 MPa and 70 °C data, the rheological properties under this condition were predicted.

The experimental data can be found in Appendix Table A1, and the temperature and pressure at the predicted point are 70 °C and 40 MPa. The first and second steps of the prediction process have been completed. Section 3.2 describes how to predict the rheometer reading at a given temperature and pressure at a certain speed. Repeat this process until readings are predicted for all speeds at the specified temperature and pressure. Through Formulas (1) and (2), the rotational speed and reading are converted into shear rate and shear stress, and the predicted results are shown in Table 7.

Table 7. Shear stress prediction results.

Shear Rate, s^{-1}	Shear Stress, Pa	Measured Shear Stress, Pa
1021.92	99.228	100.064
510.96	49.939	49.598
340.64	32.259	33.419
170.32	17.571	17.006
10.2192	4.463	4.257
5.1096	3.473	3.081

Based on the predicted shear stress, the rheological parameters and errors of the Bingham model, the Power-law model, the H-B model, the Ross model, the Carson model, and the four-parameter model were calculated using a regression method. Table 8 lists the functional forms of the six rheological models, the regression results of the rheological parameters under the predicted conditions, and the average deviation.

Table 8. Rheological optimization results.

Rheological Model	Functional Form	Rheological Parameters	Deviation, Pa
Bingham model	$\tau = \tau_0 + \mu\gamma$	$\tau_0 = 2.204$ $\mu = 0.093$	0.986
Power-law model	$\tau = K\gamma^n$	$K = 0.153$ $n = 0.93$	2.068
H-B model	$\tau = \tau_0 + K\gamma^n$	$\tau_0 = 3.385$ $K = 0.058$ $n = 1.068$	0.385
Ross model	$\tau = A(\gamma + C)^B$	$A = 0.093$ $B = 1$ $C = 23.582$	0.986
Carson model	$\sqrt{\tau} = \sqrt{\tau_c} + \sqrt{\eta_\infty}\sqrt{\gamma}$	$\tau_c = 0.209$ $\eta_\infty = 0.087$	1.752
Four parameter model	$\tau = \tau_0 + a\gamma + b\gamma^c$	$\tau_0 = 2.01$ $a = 0.094$ $b = 0.0000963$ $c = 0.09$	0.985

The Deviation of H-B model is the smallest, the value is 0.385. Therefore, the most accurate rheological model under this condition is the H-B model.

4. Model Comparison

The oil-based mud used in this paper conforms to the Bingham rheological model. Based on the experimental data, the values of plastic viscosity and static shear force at the corresponding temperature and pressure were calculated. The plastic viscosity and static shear force were predicted by the exponential model, the polynomial model, and the BP neural network, respectively.

Based on the predicted rheological parameters, the shear stress values at various rotational speeds under experimental conditions can be calculated. Due to the model established in this article directly predicting the shear stress values at six different rotational speeds, in order to compare the advantages and disadvantages of the model, the shear stress values at six different rotational speeds were calculated based on the three models.

The relationship between the shear stress predicted by different methods and the measured value is shown in Figure 7.

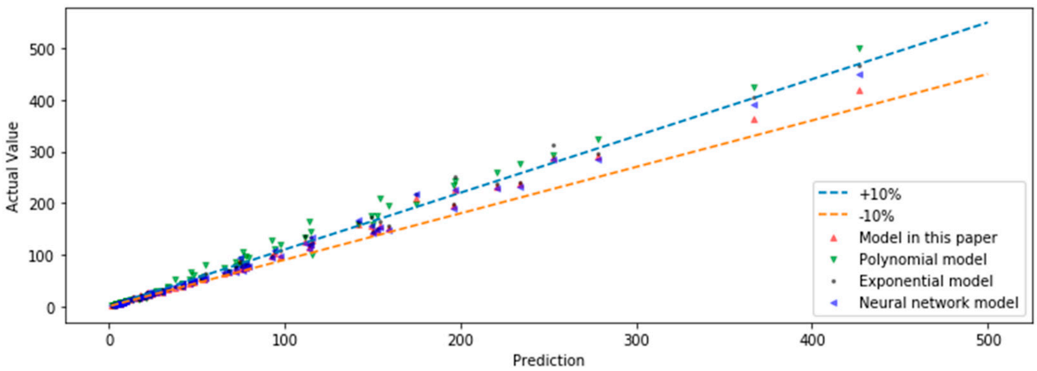

Figure 7. Comparison between predicted values and actual values of different models.

It can be seen from the figure that there are many prediction points with errors greater than 10% in the polynomial model, and the prediction points with errors greater than 10% in the polynomial model and the neural network model are significantly fewer than those in the rheological parameter model. The prediction points with errors greater than 10% in the model established in this paper are the fewest, and the whole prediction effect of the model established in this paper is the best.

At the same time, the average error of each method was calculated, and the results are shown in Figure 8.

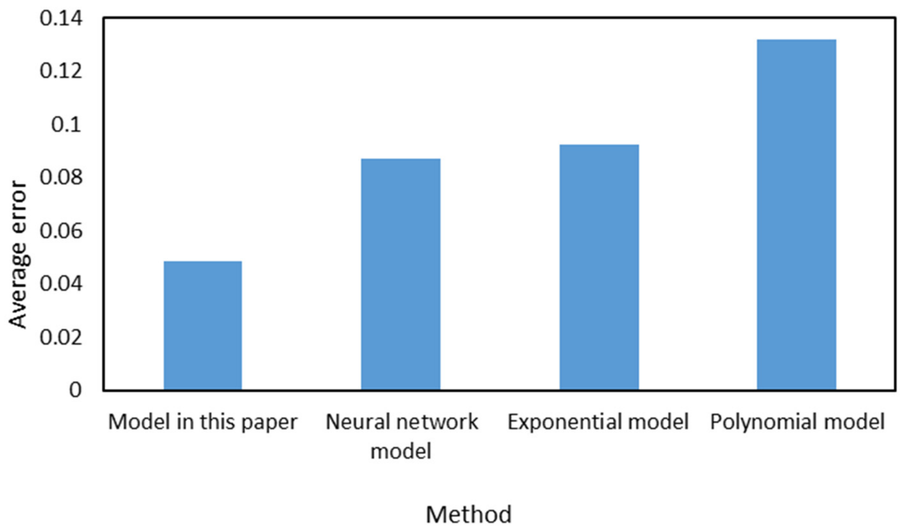

Figure 8. Error comparison chart of different methods.

It can be seen from the above figure that the average error of the polynomial model is the largest. This is because the regression law of the drilling fluid rheology in this paper is closer to the exponential model, and the polynomial regression leads to the expansion of the error. Since the neural network model does not specify the regression function, the average error is close to the exponential model. The model in this article neither specifies the rheological model at the beginning of the prediction nor the regression function form used for the prediction, so the prediction results are more in line with the actual situation and have the smallest average error. Therefore, the method established in this paper can effectively improve the accuracy of the rheological prediction of drilling fluid under high temperature and high pressure.

5. Model Application

Based on the model established in this article, the bottom hole ECD of the Hu 6 well was calculated, and the basic information of the well is shown in Tables 9–11.

Table 9. Well structure at 6880 m of the Hu 6 well.

Well Section	Top Depth, m	Bottom Depth, m	Outer Diameter, mm	Inner Diameter, mm
Casing	0	5460	273.1	245.4
Open Hole	5460	6880	241.3	—

Table 10. Drill tool assembly.

Component	Section Length, m	Inner Diameter, mm	Outer Diameter, mm
Drill pipe	2200.5	129.5	149.2
Drill pipe	4362.6	101.6	149.2
Weighted drill pipe	85.4	76.2	127
Adapter	0.5	72	158
Drill collar	27.4	57.2	158.8
Flexible joint	3.4	75	118
Jar	4.4	138	158
Drill collar	184.7	57.2	158.8
Spiral stabilizer	1.4	159	212

Table 10. *Cont.*

Component	Section Length, m	Inner Diameter, mm	Outer Diameter, mm
Drill collar	9.4	57.2	158.8
Bit	0.3	—	241.3

Table 11. Construction parameters.

Flow Rate, L/s	Standpipe Pressure, MPa	Casing Pressure, MPa
28	32	0

The bottom hole ECD values calculated based on the methods established in this article, and traditional methods are shown in Table 12 below, which also lists the bottom hole ECD values measured by PWD.

Table 12. Calculation results of circulating pressure at 6880 m of Well H.

	The Method Established in This Article, g/cm^3	Traditional Method, g/cm^3	PWD, g/cm^3
ECD	2.19	2.15	2.20

The error of the method established in this article for calculating ECD is 0.02 g/cm^3, while the traditional method is 0.06 g/cm^3. The ECD based on this method is more accurate.

6. Conclusions

Based on experiments and theoretical analysis, this paper studies the rheological properties of high-temperature and high-pressure drilling fluids and draws the following conclusions:

(1) The rheological properties of oil-based drilling fluid used in three wells in an oilfield in Xinjiang were measured via conducting experiments, and the variation law of drilling fluid under high temperature and high pressure was analyzed. When the temperature is lower than 100 °C, the shear stress decreases faster, and when the temperature is higher than 100 °C, the shear stress decreases gradually. As the pressure increases, the shear stress increases gradually. When the pressure is lower than 80 MPa, the shear stress increases more slowly, and when the pressure is higher than 80 MPa, the shear stress increases faster.

(2) This paper presents a method for directly predicting the readings of a six-speed viscometer and then optimizing the rheological model. The model reduces errors caused by prioritizing rheological models in traditional prediction methods. At the same time, in view of the fact that different drilling fluids conform to different regression functions, this paper adopts a parameter-free method for regression prediction, which expands the scope of the application of the model.

(3) The error between the shear stress and the measured value of different methods at certain shear rates was compared, and the results show that the model established in this paper had the best prediction effect and the smallest model error. This paper improves the prediction effect of oil-based drilling fluid rheology and provides theoretical support for accurate drilling hydraulic calculation.

Author Contributions: Conceptualization, Y.Y. and H.F.; methodology, Y.Y. and Y.L.; software, Y.Y.; validation, Y.Y.; data curation, Y.Y.; writing—original draft preparation, Y.Y. All authors have read and agreed to the published version of the manuscript.

Funding: Sinopec Shengli Petroleum Engineering Co., Ltd., Drilling Technology Research Institute; 10200001-22-ZC0613-0044.

Institutional Review Board Statement: Not applicable.

Data Availability Statement: Data are available on request due to restrictions, e.g., privacy or ethics.

Conflicts of Interest: The authors declare no conflict of interest.

Appendix A

Table A1. Rheological experimental data of the Tianan 1 well.

Temperature, °C	Shear Rate, 1/s	Pressure, MPa							
		0.1	10	20	40	60	80	120	150
60	1021.92	88.71471	90.57475	93.88092	112.7777	144.04068	183.45922	251.6675	276.02176
	510.96	47.28794	40.56829	45.8878	56.97139	81.82132	107.01362	155.18048	181.73715
	340.64	31.96305	25.89237	30.39939	39.57695	51.12044	72.72552	112.25137	142.57411
	170.32	18.07407	14.72702	15.71325	21.45689	26.73552	39.65871	67.48266	91.40257
	10.2192	4.07267	4.40482	4.36394	5.03846	6.51014	9.25932	14.29267	18.15583
	5.1096	3.2704	3.36749	3.53101	3.8836	4.83917	7.17955	12.21801	16.54618
70	1021.92	76.55291	77.88151	81.18257	100.06402	119.48202	142.03756	187.4859	218.03348
	510.96	36.91975	36.88909	39.58717	49.59766	58.4073	76.20032	100.44727	129.07349
	340.64	24.60976	23.1994	27.36916	33.4194	38.60605	47.97779	72.5109	89.29214
	170.32	11.87564	12.29977	13.48018	17.00608	21.31381	26.9297	38.19725	58.93363
	10.2192	3.13243	3.94492	3.92448	4.25663	4.91582	6.11156	9.23377	11.36975
	5.1096	2.15131	2.8105	3.03023	3.08133	3.85805	4.87494	6.91383	10.66968
80	1021.92	57.92185	62.15293	60.66592	78.72466	98.19376	114.6173	157.44421	194.22599
	510.96	27.33339	27.56845	30.38406	39.08128	41.63117	52.79141	77.12012	110.887
	340.64	16.6075	16.83234	22.25916	23.94035	25.27406	32.49449	50.75763	71.83638
	170.32	7.77742	9.22866	11.13469	13.66414	16.68926	17.77258	23.46512	39.41854
	10.2192	2.11554	2.86671	3.19375	3.05067	3.7814	4.1391	6.46415	9.1469
	5.1096	1.41036	2.11043	2.5039	2.47324	3.02001	3.2193	4.24641	7.13867
100	1021.92	45.55565	45.57098	47.53833	58.05471	68.11119	79.96639	113.36024	142.24707
	510.96	22.04965	22.04965	23.66952	27.86483	33.08214	40.33323	55.98516	75.02502
	340.64	14.56861	14.56861	15.6877	19.30558	21.84014	27.48669	37.78845	48.45302
	170.32	6.70943	7.63434	9.13157	11.51794	12.51439	15.4322	20.92545	27.19542
	10.2192	1.85493	2.47835	2.2484	2.45791	2.77984	3.50035	4.81362	6.16777
	5.1096	1.21618	1.74762	2.05422	2.08488	2.26373	2.79517	3.78651	4.92093
120	1021.92	37.52784	37.57894	41.85601	47.48212	56.86919	67.02787	93.74806	115.26116
	510.96	17.41488	17.41488	21.08897	24.59443	28.99925	34.29832	45.08042	58.22334
	340.64	12.06471	12.06471	14.58394	17.05718	20.24582	23.98123	31.26809	39.13238
	170.32	5.74364	6.67366	9.11624	10.16379	10.61347	14.50218	18.48798	22.1263
	10.2192	1.53811	2.05422	1.95202	2.17175	2.58055	3.05578	3.98069	4.98225
	5.1096	1.04244	1.52278	1.76806	1.8396	1.92136	2.62654	3.34705	4.00624
140	1021.92	34.5947	34.6458	32.63246	40.39966	47.68141	53.01114	73.48691	95.15331
	510.96	16.15271	16.15271	16.01474	21.4109	24.6302	28.23275	37.03217	45.90313
	340.64	11.47706	11.57926	10.50105	15.42709	17.21048	20.3378	26.63332	31.85574
	170.32	4.91582	5.24286	6.14222	8.53881	9.79076	11.67635	15.59572	17.885
	10.2192	1.46146	1.97246	1.50745	1.96224	2.19219	2.59077	3.39304	4.05734
	5.1096	0.88914	1.20085	1.3797	1.54322	1.77317	2.11554	2.82583	3.23974
160	1021.92	28.08456	28.13566	28.24808	34.6458	40.66538	43.65473	54.35507	61.93831
	510.96	12.90275	12.90275	12.22823	15.24313	17.78791	21.20139	28.18165	31.8353
	340.64	7.78764	7.9205	7.50659	10.00027	12.14136	14.43575	20.17428	21.90146
	170.32	3.42881	3.42881	3.3215	4.32306	6.84229	7.77231	11.90119	14.03206
	10.2192	0.99134	1.34904	1.07821	1.27239	1.54833	1.8396	2.57033	2.79006
	5.1096	0.61831	0.78183	0.74606	0.78183	1.23662	1.40525	2.15642	2.53967

Table A2. Rheological experimental data of the Tianwan 1 well.

Temperature, °C	Shear Rate, 1/s	Pressure, MPa							
		0.1	10	20	40	60	80	120	150
60	1021.92	83.19591	79.58825	81.46873	94.64742	120.53468	146.54969	219.97017	270.03795
	510.96	45.31548	46.73095	45.04465	53.0418	66.64462	83.84999	111.38267	143.84139
	340.64	34.78888	35.38675	36.61826	42.5152	51.77963	69.20473	97.88205	113.45733
	170.32	19.34646	18.907	20.16917	23.80238	26.12232	31.8864	47.94202	66.66506
	10.2192	3.56678	3.6281	3.75585	4.35883	5.30929	6.68388	9.26954	11.63547
	5.1096	2.7083	2.64698	2.82072	3.33172	3.96025	4.76763	6.70432	9.32575
70	1021.92	74.23808	74.42715	74.28407	87.30435	112.15939	129.52317	196.88319	233.18974
	510.96	41.12528	41.96843	40.06751	47.47701	58.50439	71.88237	96.52279	126.73311
	340.64	31.14034	31.23232	32.58136	38.55495	45.98489	56.74655	77.80997	98.28574
	170.32	16.83234	16.80168	17.07251	20.37357	23.2505	28.5138	39.77113	51.85628
	10.2192	3.19375	3.20397	3.34194	3.95514	4.71653	5.48303	7.36862	10.08203
	5.1096	2.35571	2.3506	2.38637	2.85138	3.5259	4.26174	5.56479	7.25109
80	1021.92	61.30978	62.36755	63.7217	74.73886	90.01265	111.32646	152.03272	196.05537
	510.96	30.05702	31.39584	32.27476	37.93153	45.62719	55.84719	83.30322	96.40015
	340.64	23.8126	24.76817	27.00124	31.33963	38.08483	42.6685	57.63569	73.76285
	170.32	12.26911	12.80566	14.38465	16.21914	19.55597	21.08386	29.88839	37.73735
	10.2192	2.66231	2.53967	2.76962	3.21419	3.90404	4.12377	5.45748	7.5628
	5.1096	2.02356	1.7885	2.01334	2.26884	2.9638	3.15287	4.17998	5.27863
100	1021.92	49.52612	49.52612	48.36104	57.14513	68.24916	79.55759	106.10915	129.98307
	510.96	25.7033	25.7033	24.51267	29.93438	35.35609	40.7778	52.15777	69.05654
	340.64	21.03276	21.03276	21.59486	24.75284	29.32629	32.10613	42.1064	51.68254
	170.32	11.83987	11.83987	12.35087	13.7459	15.59572	17.6295	21.40068	26.45958
	10.2192	2.15642	2.15642	2.21263	2.53967	3.00979	3.10177	3.99091	5.29907
	5.1096	1.65564	1.65564	1.72718	1.92136	2.36593	2.63676	2.99446	3.69964
120	1021.92	33.20478	33.71067	34.49761	43.75693	45.51477	58.70368	77.15078	87.66205
	510.96	18.82013	19.62751	19.48954	23.38847	24.40536	29.60223	41.39611	48.2384
	340.64	15.2789	15.81545	16.64838	17.19004	19.15228	24.71707	32.24921	36.03061
	170.32	8.687	8.90673	9.13668	10.30687	11.3953	14.82411	18.75881	20.26626
	10.2192	1.56877	1.61987	1.70674	1.76295	1.96224	2.38637	3.05578	3.69453
	5.1096	1.21618	1.24684	1.2775	1.44102	1.72718	2.06444	2.46302	2.91781
140	1021.92	26.43403	26.48513	27.53268	33.4705	40.30768	46.69007	60.26223	76.14411
	510.96	16.96009	16.97031	17.3229	20.7466	21.58975	27.6962	35.24878	42.90356
	340.64	14.39998	13.5415	15.55995	15.82056	17.69082	23.13297	30.24609	33.24566
	170.32	7.27153	8.62057	9.01915	9.30531	10.92007	13.56194	15.40154	16.70459
	10.2192	1.47679	1.38992	1.59432	1.62498	1.81405	2.23307	2.86671	3.40837
	5.1096	1.01689	1.20596	1.26217	1.30305	1.65564	2.02867	2.44769	2.64187
160	1021.92	20.26115	20.31225	20.951	27.79329	33.61869	39.98064	55.17778	68.06009
	510.96	12.59104	12.59104	12.8261	16.16293	18.97343	21.18095	28.9737	36.27589
	340.64	11.14491	11.14491	10.79743	13.28089	15.84611	18.21204	21.7175	28.37583
	170.32	5.75897	5.75897	6.09623	7.54747	8.35485	10.21489	12.14647	14.8701
	10.2192	1.14464	1.14464	1.10887	1.36437	1.62498	1.75784	2.05933	2.90759
	5.1096	0.80738	0.80738	0.85337	1.05777	1.26728	1.52789	1.70163	2.07977

Table A3. Rheological experimental data of the Hu 6 well.

Temperature, °C	Shear Rate, 1/s	Pressure, MPa							
		0.1	10	20	40	60	80	120	150
60	1021.92	59.47529	63.42021	65.35179	80.80443	98.47481	116.508	142.89604	172.19167
	510.96	35.07504	36.88398	38.39143	45.82137	56.75166	61.18714	75.39805	96.67609
	340.64	21.8197	23.61842	23.72573	27.72175	34.05304	35.82621	43.53209	55.80631
	170.32	12.43774	13.39331	14.02695	16.09139	18.94788	20.03631	23.29649	29.04013
	10.2192	2.47835	2.68275	2.69297	3.14776	3.86827	4.06756	4.94137	6.3364
	5.1096	1.95713	2.11043	2.20752	2.53456	2.98424	3.15287	3.66898	4.57345

Table A3. *Cont.*

Temperature, °C	Shear Rate, 1/s	Pressure, MPa							
		0.1	10	20	40	60	80	120	150
70	1021.92	49.99113	50.45614	51.17665	64.57507	81.38697	97.06445	115.73128	144.02024
	510.96	27.22097	26.42381	29.2292	34.4414	40.55807	46.37325	61.70325	75.51047
	340.64	17.15938	16.85278	18.69238	20.75682	24.90103	26.50557	33.75666	46.00533
	170.32	10.95584	10.70034	10.77699	12.74945	14.53284	15.82056	17.09295	21.86058
	10.2192	1.94691	1.91114	2.12065	2.35571	2.82583	3.00979	3.8325	5.22242
	5.1096	1.72718	1.6863	1.69652	2.00823	2.28928	2.48857	2.84116	3.43903
80	1021.92	43.77737	44.09419	44.76871	58.44307	69.05143	79.04659	96.84472	120.51424
	510.96	22.81615	22.22339	25.53467	29.04013	34.40563	40.23614	52.32129	65.01964
	340.64	14.80878	14.69636	16.39288	18.67705	19.68883	22.63219	30.3023	37.78334
	170.32	9.37174	9.13668	9.64257	10.81276	11.47195	12.25889	14.43064	18.56974
	10.2192	1.68119	1.67097	1.86004	2.12065	2.23818	2.57033	3.13243	4.2924
	5.1096	1.47679	1.44102	1.51767	1.70163	1.80383	1.93158	2.58055	2.92292
100	1021.92	35.40719	36.3832	36.61315	46.93024	54.07913	60.69147	68.92879	82.8842
	510.96	19.89323	20.31736	20.93056	25.96391	29.1781	31.28853	38.37099	46.41413
	340.64	12.03916	12.43263	13.07138	16.13738	17.07762	18.91722	21.02765	25.42225
	170.32	7.6139	8.38551	8.58991	9.65279	10.77699	12.2129	13.97585	15.78479
	10.2192	1.36948	1.41036	1.4819	1.83449	1.9418	2.1462	2.38637	2.88715
	5.1096	1.20085	1.2264	1.35415	1.51767	1.69652	1.92136	2.20241	2.48346
120	1021.92	25.28939	26.86327	27.63999	34.29832	38.76446	44.72783	50.11888	55.45883
	510.96	15.18181	15.51396	16.02496	20.28159	22.10075	25.27917	29.50003	32.11124
	340.64	9.58125	9.86741	10.09225	11.19601	13.04072	15.03873	17.56307	20.02098
	170.32	5.58523	6.20865	6.35684	6.97004	8.26287	9.68856	11.5997	13.72035
	10.2192	1.08843	1.11909	1.14464	1.47168	1.4819	1.70674	1.9929	2.27395
	5.1096	0.87892	0.97601	1.00156	1.25195	1.30305	1.52278	1.82427	2.16153
140	1021.92	18.89678	19.50998	22.04965	29.59201	33.39385	36.97596	43.18461	48.22307
	510.96	13.05094	13.33199	14.78834	17.79302	20.01587	22.66285	26.84794	29.86795
	340.64	8.32419	8.57969	8.93228	11.19601	12.84143	14.27223	17.04185	18.45221
	170.32	5.54435	5.74875	5.91227	7.07224	8.09424	8.6359	10.16379	11.86031
	10.2192	0.94535	0.97601	1.01178	1.27239	1.45635	1.61987	1.78339	2.0951
	5.1096	0.87381	0.90447	0.93002	1.11398	1.27239	1.35926	1.59943	1.86515
160	1021.92	14.48685	15.82567	16.27024	19.95966	23.93013	28.11522	35.44807	44.7636
	510.96	9.74988	9.93895	9.7601	12.24356	14.80367	16.863	20.71083	25.4478
	340.64	6.01958	6.45904	6.27508	7.22554	8.71255	10.09736	12.25889	13.98607
	170.32	3.70475	3.74563	3.92448	4.09822	4.81873	5.53924	7.22554	8.55414
	10.2192	0.68474	0.73073	0.71029	0.82271	0.99134	1.14464	1.38992	1.58921
	5.1096	0.58254	0.58765	0.61831	0.64386	0.75628	0.87381	1.13953	1.34904

References

1. Ansari, M.; Turney, D.E.; Morris, J.; Banerjee, S. Investigations of rheology and a link to microstructure of oil-based drilling fluids. *J. Pet. Sci. Eng.* **2021**, *196*, 108031. [CrossRef]
2. Jia, X.; Zhao, X.; Chen, B.; Egwu, S.B.; Huang, Z. Polyanionic cellulose/hydrophilic monomer copolymer grafted silica nanocomposites as HTHP drilling fluid-loss control agent for water-based drilling fluids. *Appl. Surf. Sci.* **2022**, *578*, 152089. [CrossRef]
3. Srini-Vasan, S.A.C.G. The Effect of Temperature on the Flow Properties of Clay-Water Drilling Muds. *J. Pet. Technol.* **1958**, *10*, 59–60. [CrossRef]
4. Annis, M.R. High-Temperature Flow Properties of Water-Base Drilling Fluids. *J. Pet. Technol.* **1967**, *19*, 1074–1080. [CrossRef]
5. McMordie, W.C.B.R. The Effect of Temperature and Pressure on the Viscosity of Oil-Base Muds. *J. Pet. Technol.* **1975**, *27*, 884–886. [CrossRef]
6. Politte, M.D. Invert Oil Mud Rheology as a Function of Temperature. In Proceedings of the SPE/IADC Drilling Conference, New Orleans, LA, USA, 5–8 March 1985.
7. Yan, J. Rheological properties of mineral oil mud and conventional water-in-oil emulsion mud under high temperature and pressure. *J. Pet. Univ. (Nat. Sci. Ed.)* **1989**, *5*, 18–29.
8. Yan, J. A mathematical model for predicting the apparent viscosity of water-in-oil emulsion mud. *J. Pet. Univ. (Nat. Sci. Ed.)* **1990**, *1*, 9–15.

9. Zhao, S.; Yan, J.; Shu, Y. Prediction model of rheological parameters of oil-based drilling fluid at high temperature and high pressure. *J. Pet.* **2009**, *30*, 603–606.
10. Zhao, H.; Xue, Y.; Li, G. Study on the rheology of high-temperature water-based drilling fluid at ultra-high temperature and pressure. *Pet. Drill. Technol.* **2009**, *37*, 5–9.
11. Wang, F.; Wang, R.; Liu, J. Research on the high-temperature and high-pressure rheological properties of high-density water-based drilling fluid. *J. Pet.* **2010**, *31*, 306–310.
12. Gokdemir, M.G.; Erkekol, S.; Dogan, H.A. *Investigation of High Pressure Effect on Drilling Fluid Rheology*; American Society of Mechanical Engineers (ASME): Trondheim, Norway, 2017.
13. Fakoya, M.F.; Ahmed, R.M. A generalized model for apparent viscosity of oil-based muds. *J. Pet. Sci. Eng.* **2018**, *165*, 777–785. [CrossRef]
14. Anawe, P.A.L.; Folayan, J.A. Data analyses on temperature-dependent behaviour of water based drilling fluid rheological models. *Data Brief* **2018**, *21*, 289–298. [CrossRef] [PubMed]
15. Vivas, C.; Salehi, S. Rheological investigation of effect of high temperature on geothermal drilling fluids additives and lost circulation materials. *Geothermics* **2021**, *96*, 102219. [CrossRef]
16. Agwu, O.E.; Akpabio, J.U.; Ekpenyong, M.E.; Inyang, U.G.; Asuquo, D.E.; Eyoh, I.J.; Adeoye, O.S. A critical review of drilling mud rheological models. *J. Pet. Sci. Eng.* **2021**, *203*, 108659. [CrossRef]
17. Agwu, O.E.; Akpabio, J.U.; Ekpenyong, M.E.; Inyang, U.G.; Asuquo, D.E.; Eyoh, I.J.; Adeoye, O.S. A comprehensive review of laboratory, field and modelling studies on drilling mud rheology in high temperature high pressure (HTHP) conditions. *J. Nat. Gas Sci. Eng.* **2021**, *94*, 104046. [CrossRef]
18. Alade, O.; Mahmoud, M.; Al-Nakhli, A. Rheological studies and numerical investigation of barite sag potential of drilling fluids with thermochemical fluid additive using computational fluid dynamics (CFD). *J. Pet. Sci. Eng.* **2023**, *220*, 111179. [CrossRef]